LANGMUIR

pubs.acs.org/Langmuir Article

Connecting the Non-Brownian Dots: Increasing Near-Neighbor Particle-Tracking Efficiency by Coordinate System Manipulation

José A. Epstein and Guy Z. Ramon*

Cite This: https://doi.org/10.1021/acs.langmuir.2c00584 Read Online

ACCESS | Metrics & More | Article Recommendations | Supporting Information

ABSTRACT: The nearest-neighbor algorithm (N−N) for single particle tracking (SPT) is widely employed for studying the deformation and mechanics of soft materials, or to detect flow in microfluidic systems. However, this algorithm may not perform well under certain conditions of oscillatory or directed motion of the studied tracers. Here, a method is presented with the goal of improving the performance of NN-SPT algorithms when studying directed and oscillatory motions. Specifically, the approach applies a change-of-basis matrix to the detected particles positions, prior to the calculations made by the NN-SPT algorithm. The presented results demonstrate the superior tracking efficiency when analyzing these systems, manifested via lower tracking mismatches and less spurious results than the original N−N algorithm.

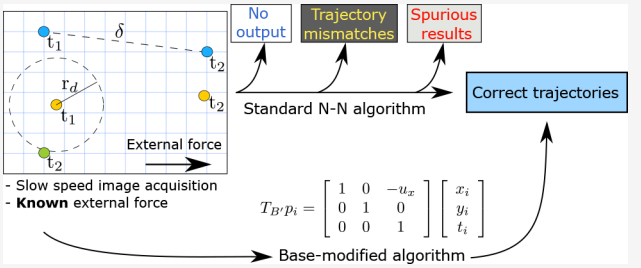

INTRODUCTION

Particle tracking algorithms are fundamental for obtaining specific quantitative data collected from imaging the motion of objects in a system of study. Still, some features in particle tracking remain an unsolved problem in the computer vision field. Specifically, available algorithms may not perform well when tracking a swarm of particles above a given particle concentration and, moreover, their performance will deteriorate when the tracked particles undergo markedly non-Brownian motion. Parameters such as light intensity, signal-to-noise ratio, and resolution are examples of variable input from video acquisition, which determine the accuracy of particle detection algorithms. In practice, monitoring a system using a camera, or detector, is stored as a video, which is comprised of a finite number of frames. In the final acquired imaging, there is a sensible tradeoff between the image quality and the total number of frames acquired during the observation time. For example, when a swarm of particles is present in the field of view, low-speed image acquisition can become detrimental to the accuracy of the particle tracking algorithm.

Multiple-object tracking algorithms usually consist of two subroutines: particle detection and particle tracking. The first subroutine is used to locate the particles in each frame of the analyzed video. Then, the tracking routine assigns an "identity" to the detected particles located in consecutive frames, usually following a criteria of proximity, to create the particle trajectories. Several methods have been proposed to address the challenges of various experimental conditions. These developments have been reviewed, discussing different approaches and abilities to overcome present issues in particle tracking (see, for example, refs 1−4).

Nearest-neighbor methods are commonly employed in particle tracking calculation routines, where possibly the most commonly employed algorithm is the code released by Crocker and Grier.[5] This method is characterized by an interactive parameter, the search radius (r_d), used to reconstruct a particle trajectory by using a threshold of radial distance when analyzing two detected particles between subsequent images. However, a high value of r_d can generate artificial jumps in the calculated particle trajectory, while a low r_d value can end up cutting a single particle trajectory into many different trajectories, recognized as many particles entering and leaving the analyzed field of view over time. Both high and low values of r_d create undesired artifacts that prevent the algorithm output from properly characterizing the real nature of the particles' motion, thereby affecting further post-analyses based on the trajectories, such as the mean square displacement (MSD) or other video-based microrheology techniques.[6−8]

The operative window at which the collected data can be effectively processed by the tracking algorithm narrows when tracking objects with directed or oscillatory motion in three dimensions (3D), using a confocal microscope. Confocal laser-scanning microscopy (CLSM) is widely used for particle tracking in two dimensions (2D) and 3D,[9,10] where the 3D

Received: March 8, 2022
Revised: July 28, 2022

images are produced by a stack of 2D images collected at various focal planes and reconstructed into a 3D image. Since this technique is slow, because of stack acquisition, when compared to the speed of the analyzed event, resonant scanning confocal laser-scanning microscopy (RS-CLSM) was developed to improve the speed of acquisition for the imaging of living or nonstatic samples. However, particle tracking experiments still encounter the limits of measurement speed for 3D scanning of thick samples (>50 μm) or 2D analysis of high tracers density or with tracers undergoing a directed motion. For 3D-imaging objects presenting a directed or oscillatory motion within a thick sample, the data processed by the algorithm may not correspond with the minimum image quality required to accurately find and locate a swarm of particles, or the minimum frame-rate required to keep a track on the particle's motion over time. Moreover, the output of a particle-tracking algorithm analyzing particles undergoing non-Brownian motion can be biased if not treated carefully, e.g., because of the selection of a a high r_d value such that it matches the requisites for a low frame rate and anisotropic motion.

Variations of a nearest-neighbor algorithm can be found in the literature, including modified features adapted to work under conditions in which the original algorithm can fail to track a single or multiple objects correctly, e.g., to study single-molecule trajectories.[11] In addition, computational strategies have been proposed and employed for solving problems of particle tracking in complex systems, using an adaptive particle search, based in the local particle density.[12] More complex algorithms were also developed, with a search radius accounting for the local particle density, as well as a motion-based search radius.[13] However, a major challenge still remains, namely the computational requirement and the accuracy of particle tracking algorithms analyzing anisotropic motion. In particular, this challenge is relevant for experiments that apply external forces on the material in which the particles are embedded or on the particles themselves, such as rheo-confocal techniques and active microrheology, respectively. Also, an applied subfield of particle-tracking—single-virus tracking—can present issues in the particle linking algorithm due to the observed anisotropic motion, where a near-neighbor algorithm is unsuitable for completing the task and a multiple-hypothesis tracking can demand large computational resources.[14]

Herein, we propose a simple, tailor-made strategy to track a swarm of particles that undergo anisotropic motion. The method is based on using a near-neighbor particle tracking algorithm and manipulating the coordinate system at which the tracking algorithm operates. Specifically, we aim to resolve issues that often emerge while tracking tracer particles that are under external forces. Therefore, we also assess which transformation matrices are optimal for particular, simple types of particle motion, where the tracked tracers exhibit an oscillatory or directed motion. The performance of the proposed algorithm is evaluated quantitatively by using a dataset of simulated particle trajectories, the ground truth (GT), which is then compared against the output from our modified algorithm and the unmodified, standard near-neighbor tracking routine.

METHODS

Particle Tracking via Spatial Manipulations. The original near-neighbor, single-particle tracking algorithm consists of two main subroutines, namely, the particle detection and the particle tracking. Once the particle-detection algorithm completes the detection of particle positions for each frame, the tracking algorithm runs over the list of detected particles, constructing the particle trajectories using, in this case, a near-neighbor method. Therein, two detected particle positions located in consecutive frames, t_i and t_{i+1}, are identified as the same entity, if their distance matches with the proximity criteria. The proximity criteria is the search radius (r_d), where this threshold is used to assign all possible combinations of nearby objects that satisfy the proximity condition, thereafter assigning the minimal distance for all particles. As illustrated in Figure 1, the selected value of r_d is dependent on the density of particles in the system, or interparticle spacing (a) and the typical displacement of a particle between frames (δ). Therefore, the optimal search radius value would fall in the range of $\delta < r_d < a/2$.[5] Moreover, the illustration in Figure 1 shows a case in which the particles exhibit a drift, as a result of which the required

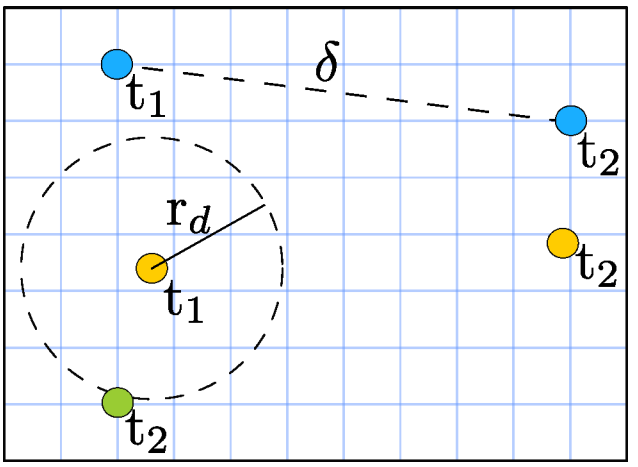

Figure 1. Illustration of an anisotropic motion. Here, the monitored particles are dominated by a horizontal, deterministic, motion when analyzing two subsequent frames, t_1 and t_2, respectively. Therefore, the criteria for assigning a search radius value, below the interparticle distance, cannot be satisfied.

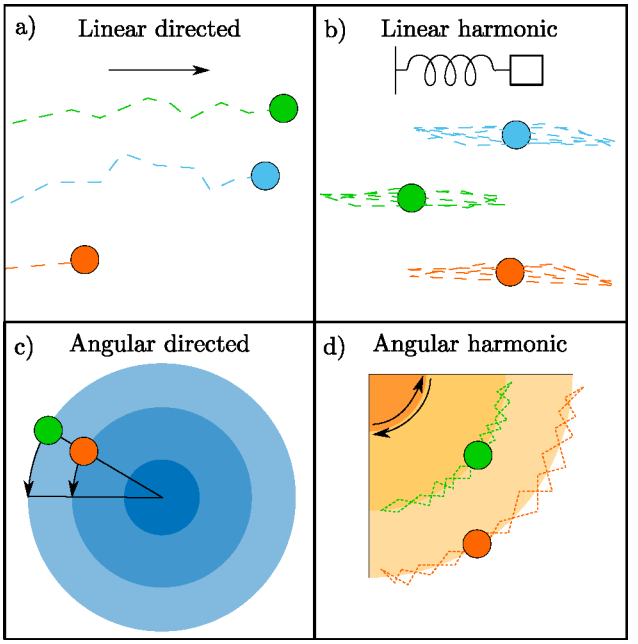

Figure 2. Illustration of the particle motion types addressed by the modified particle tracking: (a) linear directed and (2) linear harmonic; (c) angular directed and (d) angular harmonic.

https://doi.org/10.1021/acs.langmuir.2c00584
Langmuir XXXX, XXX, XXX−XXX

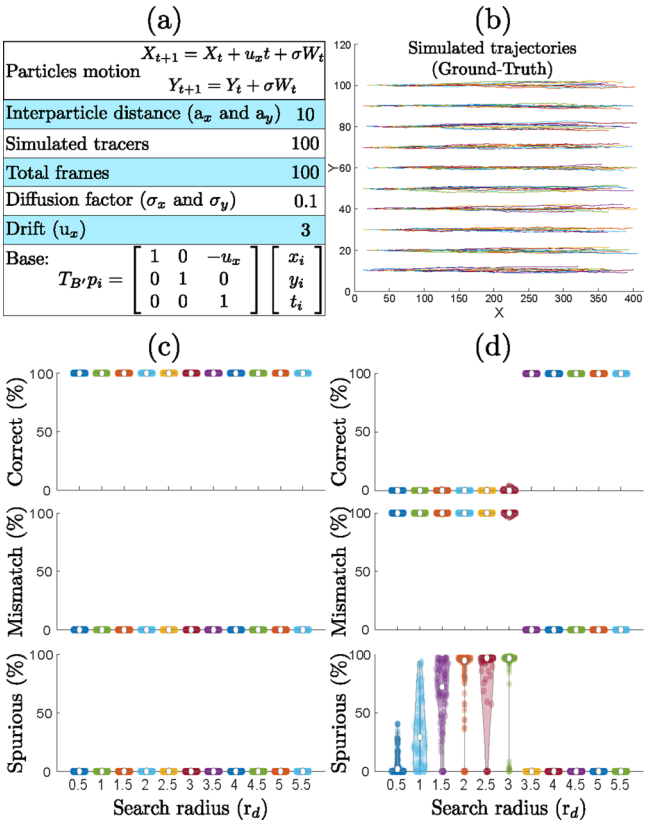

Figure 3. Tracking performance of the base-modified near-neighbor (panel (c)) versus the unmodified algorithm (panel (d)), when tracking particles moving with both a stochastic and a deterministic component (linear displacement). (a) The employed parameters for running the particles trajectories and the employed base transform. (b) The simulated trajectories in the canonical base. Panels (c) and (d) show the correctness, mismatches, and spurious results obtained by the base-modified and the unmodified algorithm, respectively, when varying the search radius (r_d).

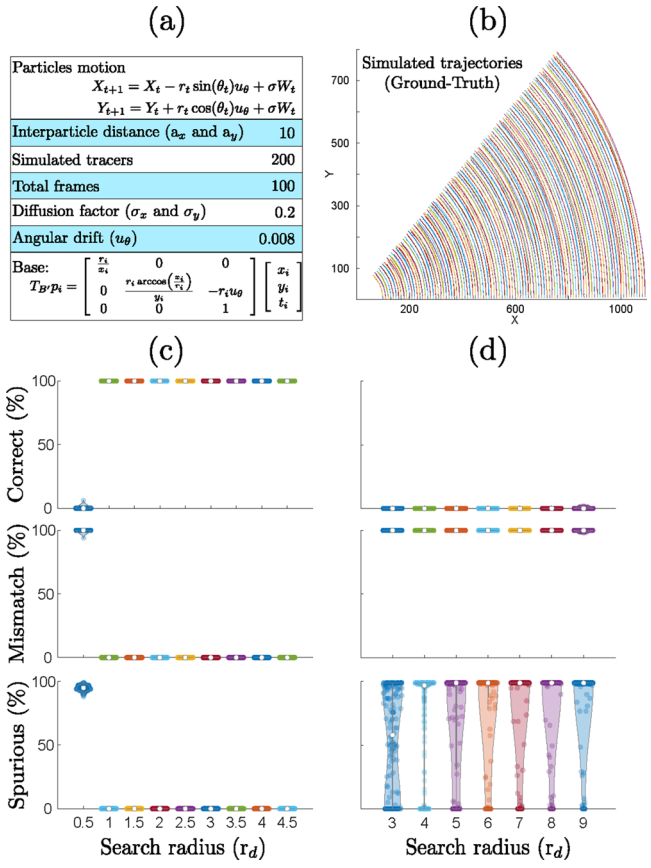

Figure 4. Tracking performance of the base-modified near-neighbor (panel (c)) versus the unmodified algorithm (panel (d)), when tracking particles moving by a stochastic and a deterministic constant-velocity angular component. (a) The employed parameters for running the particles trajectories and the employed base transform. (b) The simulated trajectories in the canonical base. Panels (c) and (d) show the correctness, mismatches, and spurious results obtained by the base-modified and the unmodified algorithm, respectively, when varying the search radius (r_d).

value of r_d cannot satisfy the optimal range condition, leading to mismatches and spurious results of the trajectories of the real particles.

The solution developed herein, for resolving the above-mentioned lower and upper contraints of the search radius, r_d, during 2D tracking is based, simply, on altering the canonical time-spatial coordinate basis ($\{1, 0, 0\}$, $\{0, 1, 0\}$, $\{0, 0, 1\}$), B, by using an alternate base (B′) to run the near-neighbor tracking algorithm. Consequently, this affects the entire list of detected coordinate tracers in each frame (x_i, y_i, t_i) for a detected particle i, $1 \leq i \leq I$, where I represents the total number of detected particles. The transformation matrix $T_{B'}$, generally expressed for 2D analyses as ($\{a_1, a_2, a_3\}$, $\{b_1, b_2, b_3\}$, $\{c_1, c_2, c_3\}$), will take specific values depending on the type of motion undergone by the analyzed particles, see Figure 2. Once the tracking analysis is complete, each position vector can be expressed back in terms of the previous coordinate basis, if necessary. Specific examples for the change of basis will be described in details in the following sections.

Adapting $T_{B'}$ To Address a Particular Motion. For particles undergoing a stochastic thermal-driven motion and, in addition, a deterministic term (u_x), which represents a particle's drift toward the positive values of the x-axis, the employed base transformation assumes the following form:

$$T_{B'}p_i = \begin{bmatrix} 1 & 0 & -u_x \\ 0 & 1 & 0 \\ 0 & 0 & 1 \end{bmatrix} \begin{bmatrix} x_i \\ y_i \\ t_i \end{bmatrix} \quad (1)$$

Experimentally, this type of motion can be observed when multiple particles are contained within a flowfield and, therefore, the tracers are advected as the whole media is in motion. Another example can be the application of external field that exerts a force on the particles themselves, directing them in an identical direction. In both cases, the suggested, modified algorithm would provide a solution for potential tracking issues. In the case where the particle motion exhibits an oscillatory term due to, e.g., an optical trap or an elastic response of the media, and assuming the harmonic term to occur along the x-axis, the proposed transformation for solution of this particle tracking problem would be a scaling matrix,

$$T_{B'}p_i = \begin{bmatrix} \frac{1}{S_x} & 0 & 0 \\ 0 & 1 & 0 \\ 0 & 0 & 1 \end{bmatrix} \begin{bmatrix} x_i \\ y_i \\ t_i \end{bmatrix} \quad (2)$$

where S_x is a scalar, an interactive input that intends to have an assigned value of $S_x > 1$, in order apply a "compressive" transformation of the axis along which the harmonic motion occurs.

The solution for tracers undergoing an angular motion can resolve issues in particle tracking during experiments using confocal rheoscopy techniques, where a custom-modified rheometer is mounted on a confocal microscope, enabling analysis of the microstructure of a soft material under shear.[15,16] In addition, the motion of tracers embedded in the soft material can be analyzed.[17−20]

https://doi.org/10.1021/acs.langmuir.2c00584
Langmuir XXXX, XXX, XXX−XXX

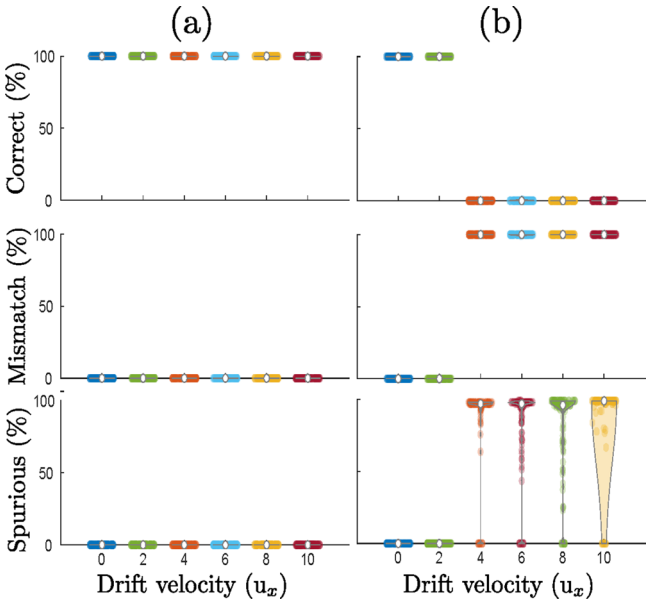

Figure 5. Tracking performance of (a) the base-modified near-neighbor versus (b) the unmodified algorithm, when tracking particles moving with both a stochastic and a deterministic component (linear displacement). Panels (a) and (b) show the correctness, mismatches, and spurious results obtained by the base-modified and the unmodified algorithm, respectively, when varying the drift velocity (u_x).

Therefore, we propose two transformations, depending on the operating mode of the rheometer: using a constant angular velocity or performing a frequency sweep. Both solutions have a transformed base coordinate of the type (r_i, $r_i\theta$, t_i),

$$T_{B'}p_i = \begin{bmatrix} \frac{r_i}{x_i} & 0 & 0 \\ 0 & \frac{r_i \arccos\left(\frac{x_i}{r_i}\right)}{y_i} & -r_i\frac{\Delta\theta}{\Delta t} \\ 0 & 0 & 1 \end{bmatrix} \begin{bmatrix} x_i \\ y_i \\ t_i \end{bmatrix} \quad (3)$$

in which the estimated value is the constant angular velocity $\left(\frac{\Delta\theta}{\Delta t}\right)$. The value r_i is the Euclidian distance calculated by the corresponding values of y_i and x_i, and

$$T_{B'}p_i = \begin{bmatrix} \frac{r_i}{x_i} & 0 & 0 \\ 0 & \frac{r_i \arccos\left(\frac{x_i}{r_i}\right)}{y_i S_{r\theta}} & 0 \\ 0 & 0 & 1 \end{bmatrix} \begin{bmatrix} x_i \\ y_i \\ t_i \end{bmatrix} \quad (4)$$

for a frequency sweep type of motion we have the interactive parameter $S_{r\theta} > 1$, which "compresses" the arc axis of the transformed space.

Tracking Performance and Efficiency. To analyze the tracking algorithm's performance, we use three qualitative categories when comparing the algorithm outcome against the ground-truth (GT) trajectories: correctness, mismatches, and spurious links. Specifically, these categories are used to evaluate each analyzed particle's GT trajectory against the output of the algorithm when tracking a swarm of particles, e.g., a 100% correct tracking would mean that the algorithm assigned the detected positions as a set of particle trajectories that are the same as the GT. The term "mismatch" is used to evaluate whether two detected positions, corresponding to two consecutive frames of a single GT trajectory, are not assigned as the same trajectory by the algorithm, since these positions are now erroneously recognized as two different particle identities. Finally, we consider the spurious track as a subcategory of mismatch, indicating that, when a mismatch is detected, the consecutive frame is also connected to a particle position that does not belong to the same GT particle identity. Therefore, a high rate of mismatches with no spurious cases will indicate that a GT trajectory is split into many artificial and smaller trajectories, and eventually into no trajectories if the mismatch is 100% and no spurious cases are indicated. For each analyzed case the results for tracking multiple particles are shown as the base-modified near-neighbor versus the unmodified algorithm (Crocker and Grier).[5] The three analyzed categories—correctness, mismatching, and spurious links—are shown for each algorithm as violin plots.[21,22]

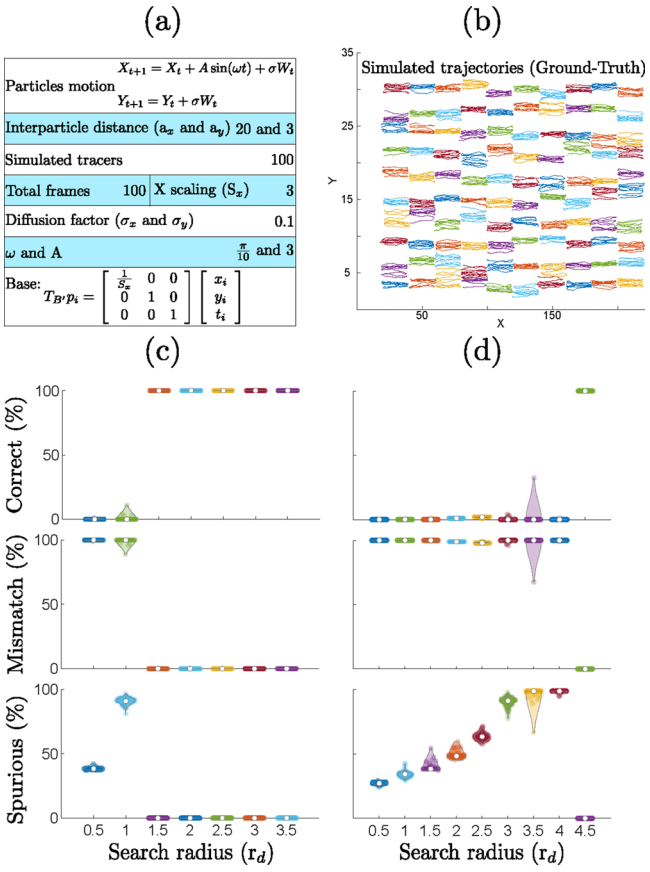

Figure 6. Tracking performance of the base-modified near-neighbor (panel (c)) versus the unmodified algorithm (panel (d)) when tracking particles moving by a stochastic and a simple harmonic component. (a) The employed parameters for running the particles trajectories and the employed base transform. (b) The simulated trajectories in the canonical base. Panels (c) and (d) show the correctness, mismatches, and spurious results obtained by the base-modified and the unmodified algorithm, respectively, when varying the search radius (r_d).

RESULTS AND DISCUSSION

Tracking Directed Motion. In our simulated datasets, tracking performance was observed to increase with the base-modified method for swarms of particles undergoing stochastic and directed motion, compared with the unmodified algorithm (see Figures 3 and 4).

In a realistic scenario, the user would need to select the translation parameter of the translation matrix, e.g., u_x for the case of linear displacement. Here, the best estimate value

https://doi.org/10.1021/acs.langmuir.2c00584
Langmuir XXXX, XXX, XXX−XXX

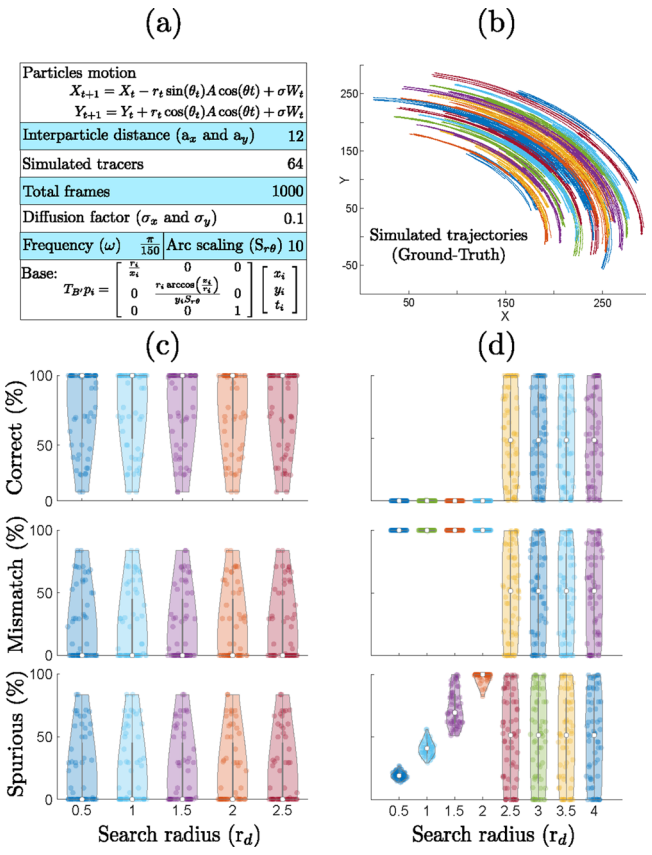

Figure 7. Tracking performance of the base-modified near-neighbor (panel (c)) versus the unmodified algorithm (panel (d)) when tracking particles moving by a stochastic and oscillatory angular component. (a) The employed parameters for running the particles trajectories and the employed base transform. (b) The simulated trajectories in the canonical base. Panels (c) and (d) show the correctness, mismatches, and spurious results obtained by the base-modified and the unmodified algorithm, respectively, when varying the search radius (r_d).

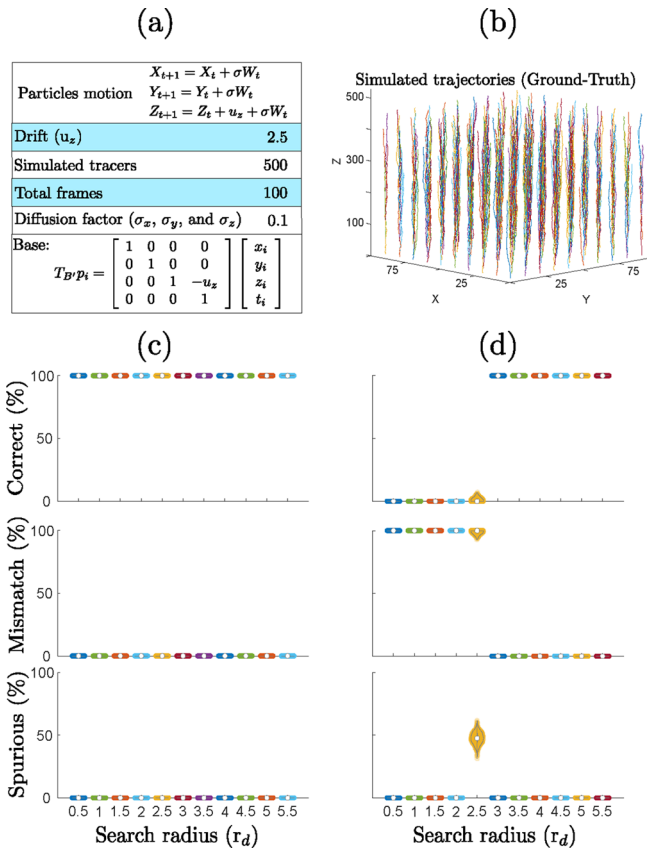

Figure 8. Tracking performance of the base-modified near-neighbor (panel (c)) versus the unmodified algorithm (panel (d)) when tracking particles moving by a stochastic and a linearly directed motion in 3D. (a) The employed parameters for running the particles trajectories and the employed base transform. (b) The simulated trajectories in the canonical base. Panels (c) and (d) show the correctness, mismatches, and spurious results obtained by employing the base modified and the unmodified algorithm, respectively, when varying the search radius (r_d).

would match with the deterministic term of the particle swarm's motion, offering the best performance. Still, a slight overestimation or underestimation of the translation parameter would present higher tracking accuracy than the unmodified algorithm. However, a considerable overshoot of the selected parameter would play to the detriment of the tracking algorithm, decreasing its efficiency compared to the unmodified algorithm. For example, a 200% drift term, u_x, in the transformation matrix $T_{b'}$ would correspond with a scenario where the modified algorithm would conclude that the original system is moving in the opposite direction, in which case both algorithms would exhibit no difference in the tracking accuracy.

The improvement in the algorithm arises from the fact that the closer the selected parameter u_x is to the particle swarm's deterministic term, the more the optimal cutoff for selecting r_d approaches $\sigma W_t < r_d < a/2$. Here, W_t is a normal distributed random variable with zero mean and unit variance.

To further study the efficiency of this method under scenarios of anisotropic motion, the method is evaluated by varying the drift velocity (u_x) of linear-directed particle motions, see Figure 5. Here, the same initial parameters are simulated as presented in Figure 3, in this case, varying (u_x).

The results show the base-modified method to present a high particle-tracking efficiency for the studied scenarios. The simple N−N method works correctly for relative low (u_x) values; however, its tracking efficiency abruptly decreases for drift values above 4. Tracking mismatches and spurious results can further lead to an erroneous characterization of the nature of the observed particle motion. To observe the errors that tracking mismatches can lead to in more detail, see Figures S.1 and S.2 in the Supporting Information.

Tracking Harmonic Motion. The simulated trajectories containing harmonic motion were also analyzed by both algorithms. The tracking performance was also observed to increase with the proposed method, compared with the standard N−N algorithm (see Figures 6 and 7). However, the transformation matrices accounting for translation, employed to track drifting particles, were found to be more accurate than scaling matrices, employed to track particles undergoing harmonic motion. The difference lies in the fact that the optimal cutoff parameters for tracking using translation matrices is $\sigma W_t < r_d < a/2$, for the type of motion we analyzed. However, the scaling matrices are still dependent on the amplitude term of the harmonic motion, $(\sigma_x W_t + A) < r_d < a_x/2$ and $(\sigma_\theta W_t + r_t \cos(\theta_t)A) < r_d < a_{r\theta}/2$, for the simple harmonic and angular harmonic motion, respectively.

https://doi.org/10.1021/acs.langmuir.2c00584
Langmuir XXXX, XXX, XXX−XXX

A space-transformed particle tracking routine can enhance the tracking output, when employed properly with a transformation matrix that addresses the anisotropic motion present in the analyzed system. This prevents the generation of spurious data, since, in practice, a high rate of tracking mismatches with no spurious cases represents an easy scenario for a user to recognize issues in the output, e.g., by noticing the presence of many short trajectories when compared to the amount of particles present in the FOV during the acquisition, or even when no trajectories at all are generated. Under such obvious conditions of data misinterpretation, the user will probably rerun the code using a higher r_d threshold value.

However, a high rate of spurious cases would require a more-detailed analysis by the user, since it will not necessarily indicate a suspicious number of trajectories in the output. In fact, a 100% spurious tracking would generate the same amount of trajectories as listed in the GT. To recognize this type of error, the end user would also need to analyze the generated trajectories, looking for spurious linking.

Potential Applications in 3D Video: Tracking Transport of Particles. The proposed method may be interesting for solving problems in particle tracking experiments that require 3D resolution of trajectories while, in addition, the monitored system undergoes an abrupt variation of particle positions due to compaction or transport (e.g., a flow field). Particularly, particle tracking in this type of experiment can be limited by the imaging acquisition speed, for example when employing 3D imaging made of Z-stacks of 80−200 μm width by using confocal microscopy. For this case, the imaging speed may force the required r_d to be a value that does not satisfy the $r_d < a/2$ condition. Here, the proposed method was evaluated against the unmodified algorithm (standard Crocker and Grier),[5] as shown in Figure 8, using an equal initial interparticle distance for the axis, $a_x = a_y = 10$, and $a_z = 50$. As was shown for the 2D case, these results also demonstrated the translation base-modified N−N algorithm to have higher accuracy when tracking particles undergoing this type of motion.

CONCLUSIONS

Herein, we presented a simple strategy for tracking swarms of particles moving with both deterministic and stochastic components, by using a N−N tracking algorithm and transforming the space in which the particles are monitored and detected. The performance analysis of the proposed algorithm revealed an enhanced accuracy when compared to the standard N−N algorithm.

Employing an algorithm that properly addresses the tracking issues of particles undergoing Brownian motion and external forces enhances the accuracy of posterior calculation of the mean square displacement (MSD), which is used to evaluate the type of particle motion and extract micromechanical properties of samples.[23] The improvement is due to reduced mismatches and spurious tracks in the algorithm outcome, resulting in a clearer picture of the particles trajectories.

ASSOCIATED CONTENT

Supporting Information

The Supporting Information is available free of charge at https://pubs.acs.org/doi/10.1021/acs.langmuir.2c00584.

Detailed description of the particle motion employed to generate different particle trajectories; performance of the base-modified modified algorithm versus simple N−N when varying the drift velocity (u_x) (Figure S1); distribution of the calculated particle displacements obtained by both algorithms, showing how incorrect tracking can lead to further errors in the motion analysis of the observed particles (Figure S2); base-modified algorithm efficiency when varying the estimated value of u_x (Figure S3); conditions studied in Figure 5, adding more detail regarding the region at which the N−N algorithm starts to fail (Figure S4) (PDF)

AUTHOR INFORMATION

Corresponding Author

Guy Z. Ramon − *Department of Civil & Environmental Engineering and Wolfson Department of Chemical Engineering, Technion - Israel Institute of Technology, Haifa 32000, Israel;* orcid.org/0000-0002-0711-0654; Email: ramong@technion.ac.il

Author

José A. Epstein − *Department of Civil & Environmental Engineering, Technion - Israel Institute of Technology, Haifa 32000, Israel*

Complete contact information is available at: https://pubs.acs.org/10.1021/acs.langmuir.2c00584

Notes

The authors declare no competing financial interest.

ACKNOWLEDGMENTS

The research was supported by the Israel Science Foundation (Grant No. 3041/21).

REFERENCES

(1) Saxton, M. J. Single-particle tracking: connecting the dots. *Nat. Methods* **2008**, *5*, 671−672.

(2) Kalaidzidis, Y. Multiple objects tracking in fluorescence microscopy. *J. Math. Biol.* **2009**, *58*, 57−80.

(3) Meijering, E.; Dzyubachyk, O.; Smal, I. *Methods in Enzymology*, 1st Edition; Elsevier, 2012; Vol. *504*, pp 183−200.

(4) Smal, I.; Meijering, E. Quantitative comparison of multiframe data association techniques for particle tracking in time-lapse fluorescence microscopy. *Med. Image Anal.* **2015**, *24*, 163−189.

(5) Crocker, J.; Grier, D. Methods of Digital Video Microscopy for Colloidal Studies. *J. Colloid Interface Sci.* **1996**, *179*, 298−310.

(6) Josephson, L. L.; Furst, E. M.; Galush, W. J. Particle tracking microrheology of protein solutions. *J. Rheol.* **2016**, *60*, 531−540.

(7) Sonn-Segev, A.; Bernheim-Groswasser, A.; Diamant, H.; Roichman, Y. Viscoelastic response of a complex fluid at intermediate distances. *Phys. Rev. Lett.* **2014**, *112*, 1−5.

(8) Schuster, B. S.; Suk, J. S.; Woodworth, G. F.; Hanes, J. Nanoparticle diffusion in respiratory mucus from humans without lung disease. *Biomaterials* **2013**, *34*, 3439−3446.

(9) Weeks, E. R.; Crocker, J. C.; Levitt, A. C.; Schofield, A.; Weitz, D. A. Three-dimensional direct imaging of structural relaxation near the colloidal glass transition. *Science* **2000**, *287*, 627−631.

(10) Cang, H.; Wong, C. M.; Xu, C. S.; Rizvi, A. H.; Yang, H. Confocal three dimensional tracking of a single nanoparticle with concurrent spectroscopic readouts. *Appl. Phys. Lett.* **2006**, *88*, 223901.

(11) Anthony, S.; Zhang, L.; Granick, S. Methods to track single-molecule trajectories. *Langmuir* **2006**, *22*, 5266−5272.

(12) Mazzaferri, J.; Roy, J.; Lefrancois, S.; Costantino, S. Adaptive settings for the nearest-neighbor particle tracking algorithm. *Bioinformatics* **2015**, *31*, 1279−1285.

(13) Jaqaman, K.; Loerke, D.; Mettlen, M.; Kuwata, H.; Grinstein, S.; Schmid, S. L.; Danuser, G. Robust single-particle tracking in live-cell time-lapse sequences. *Nat. Methods* **2008**, *5*, 695−702.
(14) Liu, S. L.; Wang, Z. G.; Xie, H. Y.; Liu, A. A.; Lamb, D. C.; Pang, D. W. Single-Virus Tracking: From Imaging Methodologies to Virological Applications. *Chem. Rev.* **2020**, *120*, 1936−1979.
(15) Dutta, S. K.; Mbi, A.; Arevalo, R. C.; Blair, D. L. Development of a confocal rheometer for soft and biological materials. *Rev. Sci. Instrum.* **2013**, *84*, 063702.
(16) Arevalo, R. C.; Kumar, P.; Urbach, J. S.; Blair, D. L. Stress heterogeneities in sheared type-i collagen networks revealed by boundary stress microscopy. *PLoS One* **2015**, *10*, e0118021.
(17) Basu, A.; Wen, Q.; Mao, X.; Lubensky, T. C.; Janmey, P. A.; Yodh, A. G. Nonaffine displacements in flexible polymer networks. *Macromolecules* **2011**, *44*, 1671−1679.
(18) Wen, Q.; Basu, A.; Janmey, P. A.; Yodh, A. G. Non-affine deformations in polymer hydrogels. *Soft Matter* **2012**, *8*, 8039−8049.
(19) Boitte, J. B.; Vizcaïno, C.; Benyahia, L.; Herry, J. M.; Michon, C.; Hayert, M. A novel rheo-optical device for studying complex fluids in a double shear plate geometry. *Rev. Sci. Instrum.* **2013**, *84*, 013709.
(20) Boukany, P. E.; Wang, S.-Q.; Ravindranath, S.; Lee, L. J. Shear banding in entangled polymers in the micron scale gap: a confocal-rheoscopic study. *Soft Matter* **2015**, *11*, 8058−8068.
(21) Hintze, J. L.; Nelson, R. D. Violin plots: A box plot-density trace synergism. *Am. Stat.* **1998**, *52*, 181−184.
(22) Bechtold, B. *Violin Plots for Matlab*, 2016. Available via the Internet at: https://github.com/bastibe/Violinplot-Matlab (accessed April 2020).
(23) Dunderdale, G.; Ebbens, S.; Fairclough, P.; Howse, J. Importance of particle tracking and calculating the mean-squared displacement in distinguishing nanopropulsion from other processes. *Langmuir* **2012**, *28*, 10997−11006.

https://doi.org/10.1021/acs.langmuir.2c00584
Langmuir XXXX, XXX, XXX−XXX